Development 134, 1643-1652 (2007) doi:10.1242/dev.003533

Novel receptor-like kinase ALE2 controls shoot development by specifying epidermis in *Arabidopsis*

Hirokazu Tanaka[1,*], Masaru Watanabe[2], Michiko Sasabe[2], Tomonori Hiroe[2], Toshihiro Tanaka[2], Hirokazu Tsukaya[3], Masaya Ikezaki[2], Chiyoko Machida[1] and Yasunori Machida[2,†]

The epidermis plays crucial roles in the development of various organs and in water retention in both animals and plants. In *Arabidopsis thaliana*, the subtilase ABNORMAL LEAF SHAPE 1 (ALE1) and the *Arabidopsis* homolog of the Crinkly4 (ACR4) receptor-like protein kinase (RLK) have been implicated in the intercellular communication that is required for surface functions of the epidermis. We have identified a novel mutant gene in *Arabidopsis*, *ale2*, which is associated with various epidermal defects, including disorganization of epidermis-related tissues, defects in the leaf cuticle and the fusion of organs. *ALE2* encodes a previously uncharacterized RLK with a cluster of basic amino acid residues followed by a cysteine-containing sequence in the putative extracellular domain. Our genetic investigations suggest that ALE2 and ACR4 function in the same process, whereas ALE1 has a different mode of action, and that these three genes play partially overlapping roles in positively regulating protoderm-specific gene expression and for the formation of leafy organs. We propose that at least two modes of intercellular communication facilitate the specification of epidermis, thereby promoting shoot organogenesis in *Arabidopsis*.

KEY WORDS: Intercellular signaling, Epidermis, Tissue specification, Embryonic patterning, *Arabidopsis*

INTRODUCTION

In multicellular organisms, including in animals and higher plants, the epidermis differentiates during embryogenesis and supports the further development and survival of adult organisms. In animals, cells ingress from the surface into the interior of the embryo during gastrulation to generate outer (ectoderm) and inner (mesoderm and endoderm) fields, which serve as germ layers. Subsequently, an alternative cell-fate specification, either into neural or epidermal tissue, takes place in the ectoderm. Specification of the epidermis requires the activities of: the bone morphogenetic protein (BMP) pathway, involving extracellular regulators such as subtilisin-like proteases; BMPs cleaved by the proteases; and receptor kinases (Cui et al., 1998; Stern, 2005).

In higher plants, specification of outer (protoderm) and inner (provascular and ground) tissues takes place during early embryogenesis in a way that is apparently different from the mechanisms involved in animal systems; the tissue specification in higher plants does not involve cell ingression (Esau, 1977; Jürgens and Mayer, 1994; Ito et al., 2002). Instead, in both monocotyledonous and dicotyledonous plants, cells at the outermost part of the early embryo, via currently unknown mechanism(s), acquire distinct characteristics, including the formation of epidermal cuticle and of a regulated cell-division plane perpendicular to the surface of the embryo (anticlinal division), which enables self-maintenance of the protodermal cell-layer that generates cuticle. During post-embryonic development, epidermal cells of most aerial organs are derived from the protoderm of the shoot apical meristem (SAM; L1 layer) (Satina et al., 1940).

[1]College of Bioscience and Biotechnology, Chubu University and CREST, Japan Science and Technology Agency, 1200 Matsumoto-cho, Kasugai 487-8501, Japan. [2]Division of Biological Science, Nagoya University, Nagoya 464-8602, Japan. [3]Center for Integrative Bioscience, National Institute for Basic Biology, Okazaki 444-8585, Japan.

*Present address: ZMBP, Entwicklungsgenetik, Universität Tübingen, D-72076 Tübingen, Germany
†Author for correspondence (e-mail: yas@bio.nagoya-u.ac.jp)

Accepted 25 February 2007

In *Arabidopsis thaliana*, the first indication of the morphological differentiation of the protoderm is visible in the embryo at the 16-cell stage, when outer and inner cells are generated (Jürgens and Mayer, 1994). Outermost cells of early embryos express a specific set of genes, which include those for homeodomain transcription factors (*ATML1* and *PDF2*) (Lu et al., 1996; Abe et al., 2003), for fatty-acid metabolism (*FDH*) (Yephremov et al., 1999), for a putative extracellular protein (*PDF1*) (Abe et al., 1999) and for a receptor-like protein kinase (RLK; *ACR4*) (Tanaka et al., 2002; Gifford et al., 2003). The homeodomain proteins ATML1 and PDF2 are essential for the differentiation of the epidermis, the expression of *PDF1* and *ACR4* in seedlings (Abe et al., 2003), and for maintaining *ATML1* promoter activity (Takada and Jürgens, 2007). ATML1 and PDF2 proteins bind to a *cis*-regulatory element, the L1 box, which is found in protoderm-specific genes such as *PDF1* and *FDH*, as well as in the genes for ATML1 and PDF2 themselves (Abe et al., 2001; Abe et al., 2003). Thus, it seems possible that the expression of protoderm-specific genes involves positive-feedback regulation by ATML1 and PDF2. Our understanding of the regulatory mechanisms that control the activity and/or expression of ATML1 and PDF2 is, however, very limited.

We have shown that the *abnormal leaf shape 1* (*ale1*) mutation in *Arabidopsis* results in impaired cuticle formation, in the adhesion of endosperm and embryo, and in the fusion of cotyledons and leaves (Tanaka et al., 2001). The *ALE1* gene encodes a member of the subtilisin-like serine protease family and is preferentially expressed within the endosperm (Tanaka et al., 2001). These observations imply that a signal from the endosperm is required for the formation of cuticle around the embryo. Mutations in the *ACR4* gene, which encodes a RLK, affect the organization of cell layers in ovules and at sepal margins, as well as affecting cuticle formation in leaves and ovules (Gifford et al., 2003; Watanabe et al., 2004). Thus, signaling systems that include the subtilisin-like serine proteases and RLKs have been shown to be involved in epidermal differentiation in both animal and plant embryos, yet our understanding of this signaling pathway in plants is still very limited.

We isolated a novel *Arabidopsis* mutant, designated *abnormal leaf shape 2* (*ale2*), which has epidermal defects similar to those of *ale1* and/or *acr4* mutant plants. We describe here the molecular cloning of the *ALE2* gene and show that it encodes a novel RLK. Our genetic analysis revealed that *ALE2*, *ALE1* and *ACR4* play collectively essential roles in protoderm specification, and in the formation of the primordia of cotyledons, during embryogenesis. Furthermore, our results suggest that ALE2 and ACR4 act in close harmony whereas ALE1 functions in a different manner to ensure robust facilitation of the differentiation of plant epidermis.

MATERIALS AND METHODS

Plant materials and growth conditions

Arabidopsis mutant lines *ale1-1*, *ale1-2*, *acr4-1* and *acr4-5* have been described previously (Tanaka et al., 2001; Watanabe et al., 2004). The *ale2-1* mutant was isolated from a T-DNA-tagged population with a Columbia-6 background (http://www.arabidopsis.org/abrc/jack.jsp). Lines were backcrossed at least three times with a wild-type strain [Columbia (Col-0), Landsberg *erecta* (L*er*) or Wassilewskija (Ws)], as indicated in the text and Figures. The *ale2-2* mutant was isolated by reverse-genetic screening of a T-DNA-tagged population, generated at the University of Wisconsin (Krysan et al., 1996), with following gene specific primers: UWBC-ALE2#1, 5′-GAGGAAGCTATATGGTTACACCTTTGGTT-3′; and UWBC-ALE2#4, 5′-ACCGGAAATCTTTACCCAGATGAACCGAA-3′. Plants were grown as described elsewhere (Tanaka et al., 2004b).

Analysis of cuticle defects

To assess the permeability to water-soluble molecules of the leaf surface, we immersed plantlets in an aqueous solution of toluidine blue (TB test), as described by Tanaka et al. (Tanaka et al., 2004b). For quantification of the amount of TB bound to plant tissues, the aerial parts of each plant were washed and ground thoroughly in a microtube that contained 200 μl of buffer [200 mM Tris-HCl (pH 8.0), 250 mM NaCl, 25 mM EDTA]. Next, 400 μl of ethanol was added, with vortex mixing, and plant debris was pelleted by centrifugation. The supernatant was examined spectrophotometrocally and the amount of TB was determined by the absorbance at 630 nm (A_{630}). The major peak of absorbance due to plant material (A_{435}) was used for normalization. Relative levels of TB were calculated as the ratio of A_{630}:A_{435}. When it was necessary to determine the genotype of a particular plant (e.g. to identify a segregating *ale2* mutation), DNA was extracted from the pellet. Transmission electron microscopy was performed as described previously (Watanabe et al., 2004).

Cloning and sequencing of the *ALE2* gene

An F_2 mutant population was generated by genetic crossing of *ale2-1* (isolated in ecotype Col) and L*er*. Rough mapping of *ALE2* was performed with CAPS and SSLP markers, available from TAIR (http://www.arabidopsis.org). CAPS markers between *PHYB* and *ER* were designed on the basis of information from the CEREON collection of polymorphisms (http://www.arabidopsis.org/Cereon/index.jsp). Meiotic-recombination breakpoints were generated near *ALE2* by screening 142 *ale2* mutants in the F_2 generation for recombinants between the *ale2-1* mutation and flanking markers. The interval of recombination breakpoints closest to the *ale2* mutation was narrowed down to a 55 kb region that was located on one BAC (F11A3). Overlapping DNA fragments covering this region were amplified from *ale2-1* genomic DNA by PCR and DNA sequences were determined with automated sequencers (ABI3100; Applied Biosystems). Reverse transcriptase (RT)-PCR was performed as described previously (Watanabe et al., 2004). *ALE2* cDNA, covering the entire coding region, was amplified with primers ALE2RT-5′ (5′-GAGGCTTGGTGTCTCCGTTATTGACTAAT-3′) and ALE2RT-3′ (5′-CCTCCTTTTCCCTTTTCTTC-3′) and cloned into pBluescript SK (–) (Stratagene), and its nucleotide sequence was determined. For the complementation experiment, a fragment of genomic DNA covering the entire coding region of *ALE2* (nucleotides –2179 to 4389 relative to the initiation codon) was cloned into the binary vector pGreen0029 (Hellens et al., 2000) (http://www.pgreen.ac.uk/) and introduced into *ale2-1*/+ plants by *Agrobacterium*-mediated transformation.

Kinase assays in vitro

An *ALE2* cDNA fragment encoding the protein kinase domain (residues 324-619) was PCR amplified and cloned into the GST fusion vector pGEX4T-3 (Amersham Pharmacia Biotech). To generate kinase-inactive ALE2, a cDNA fragment corresponding to residues 289-619 was PCR amplified, a point mutation at the 377th codon (AAA to TGG) was introduced with mutagenic primers, and this fragment was then cloned into the pGEX4T-3 vector. An *ACR4* cDNA fragment encoding the protein kinase domain (Watanabe et al., 2004) was cloned into the NusA fusion vector pET50 (Novagen). Recombinant proteins (1 μg each) and myelin basic protein (MBP; 10 μg) was incubated in 20 μl of kinase buffer (Sasabe et al., 2006) containing 50 μM ATP and 10 μCi of [γ-^{32}P] ATP. The reaction products were then separated by SDS-PAGE on polyacrylamide gels.

Histological analysis

For observations of cell morphology, we prepared semi-thin sections (500 nm thickness) as described previously (Watanabe et al., 2004). Morphology of ovules and embryos were examined as described by Tanaka et al. (Tanaka et al., 2004a).

Analysis of patterns of gene expression

In situ hybridization was performed essentially as described previously (Tanaka et al., 2001). Template DNA for transcription in vitro was amplified by RT-PCR and cloned into the *Eco*RV site of pBluescript SK (–). For *ATML1*, we used primers ATML1-5′D (5′-AGCCTAAGACCAAGTCC-GAT-3′) and ATML1-3′U (5′-CCAGTAGTAGTAACCACTTCAAGA-3′) for RT-PCR, and we cloned the product of PCR into the vector to generate pNU562. For *FDH*, we used primers FDH-5′D (5′-CGGTGAACTTGAAGTACGTGA-3′) and FDH-3′U (5′-ACAC-GTGTCTTCTCGAAGAGTT-3′), generating plasmid pNU823. For *PDF1*, we used primers PDF1-5′D (5′-CGTAAGGTTTGAGGATGCCA-3′) and PDF1-3′U (5′-TCCAAGCAAGCCCCATATCA-3′) to generate pNU563. We generated an antisense probe for *ATML1* by linearizing pNU562 with *Hin*dIII, with subsequent synthesis of RNA by T3 RNA polymerase. We generated an antisense probe for *FDH* by linearizing pNU823 (*FDH*) with *Cla*I, with subsequent transcription by T3 RNA polymerase. For the *PDF1* probe, we digested pNU563 with *Sma*I and transcribed the probe with T7 RNA polymerase. For fusion of the *PDF1* promoter (p*PDF1*) with a gene for green fluorescent protein (*GFP*), a 1595 bp fragment (nucleotides –1602 to –8 relative to the initiation codon) containing the *cis*-regulatory sequence of the *PDF1* gene (Abe et al., 1999) was amplified by PCR and cloned upstream of *sGFP(S65T)* (Chiu et al., 1996) in pGreen. Two independent transgenic lines (ecotype L*er*) were crossed with *ale1-1; ale2-1*/+ plants and the fluorescence due to GFP was examined under a fluorescence stereomicroscope.

RESULTS

Phenotype of *ale2* mutants

The *ale2* mutation was identified by genetically screening for mutations associated with irregular leaf morphology. Homozygous *ale2* plants produced irregularly malformed leaves with eventual leaf fusion, as shown in Fig. 1C. In addition, the *ale2* mutant leaves exhibited increased permeability to toluidine blue (TB) compared with wild-type leaves, suggesting that defects in cuticle on the plant surface were present (Fig. 1D). These epidermal and morphological defects were associated with a recessive mutation.

At the reproductive stage, *ale2* plants generated malformed and fused floral organs (Fig. 1E). In addition, *ale2* plants were sterile. Reciprocal crosses between *ale2* and wild-type plants indicated that sterility was mainly due to defects in female reproductive tissue(s), although male fertility was also reduced. Therefore, we maintained *ale2* mutants as the self-progeny of heterozygous plants or via genetic crosses with pollen from homozygous

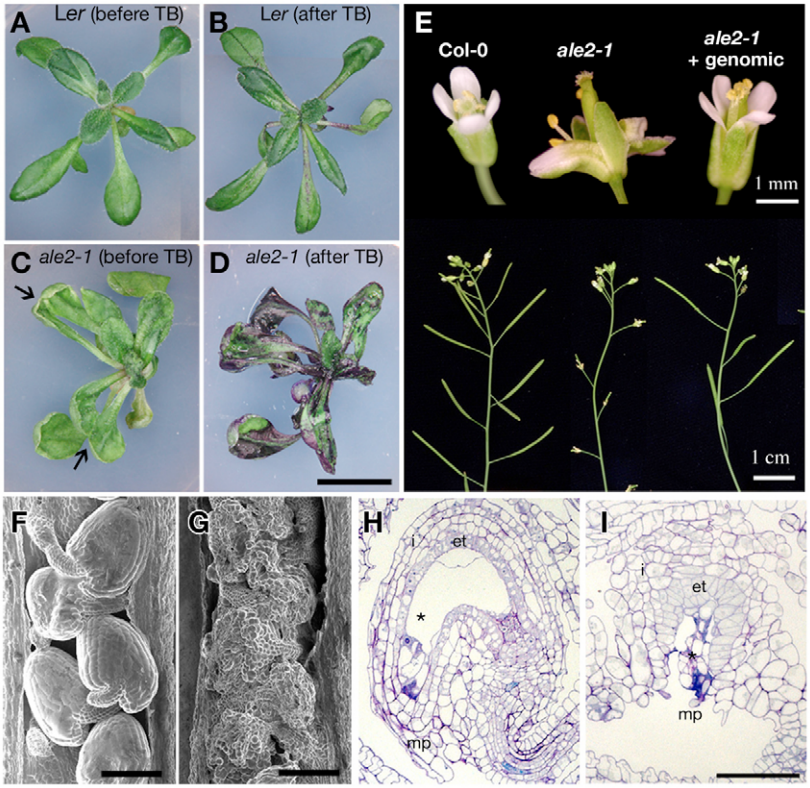

Fig. 1. The *ale2* mutant is defective in surface functions and in the organization of epidermis-related tissues. (**A**,**C**) Gross morphology of 18-day-old plants. Arrows indicate fusion of leaves. (**B**,**D**) Defects on the surface of the epidermis, as revealed by the TB test. (**E**) Morphology of flowers and inflorescences of a wild-type plant (left; Col-0), an *ale2-1* plant (middle) and an homozygous *ale2-1* plant that harbored a 6.5 kb *ALE2* transgene (right). (**F**,**G**) Scanning electron micrographs of mature wild-type (F) and *ale2-1* (G) ovules. The *ale2-1* ovules have a rough surface and have fused to one another. (**H**,**I**) Sections of mature wild-type (H) and *ale2-1* (I) ovules. Asterisk indicates the embryo sac. i, integument; et, endothelium; mp, micropyle. Scale bars: 1 cm in D for A-D; 100 μm in F,G; 100 μm in I for I,H.

parents. In order to identify the primary defect responsible for the female sterility of *ale2* plants, we examined the morphology of female gametophytes (ovules). Ovules from wild-type parents were oval with a smooth surface (Fig. 1F), reflecting the organized development of flattened layers of epidermal cells. The inner cells – including the adaxial outer integumental cells, inner integumental cells and endothelial cells – are derived from the protoderm (L1 layer) (Jenik and Irish, 2000) and form organized layers (Fig. 1H) that cover the female gametes (embryo sacs; Fig. 1H, asterisk). Scanning electron microscopy revealed that adjacent ovules generated from *ale2* parents had fused to one another. Moreover, their surfaces were rough and disorganized as a consequence of the swollen outer cells (Fig. 1G). Histological analysis confirmed that organization in the integument and endothelium had been disturbed by the *ale2* mutation, which had induced irregularly orientated cross walls and the deformation of cells (Fig. 1I). In addition, mature ovules from *ale2* plants contained degenerated embryo sacs (Fig. 1I), suggesting that the sterility of *ale2* plants was due, at least in part, to the failure of ovules to develop. These observations suggested that the *ALE2* gene is involved in the regulation of cell morphology, of the plane of cell division and of cuticle formation in epidermis-related tissues.

The *ALE2* gene encodes a novel receptor-like protein kinase

Using a map-based approach, we narrowed down the region that contained the *ale2* mutation to a 55 kb region, as shown in Fig. 2A. We determined the nucleotide sequence of the entire 55 kb region from the *ale2-1* mutant and compared this sequence with that of the wild type (Col-0). The only difference was the insertion of a single nucleotide, and this insertion was located within a putative gene (At2g20300). Subsequent amplification by reverse transcriptase (RT)-PCR, determination of the cDNA sequence, and comparison of the cDNA and the corresponding genomic DNA sequences indicated that the At2g20300 gene consists of eight exons, with an open reading frame of 2232 base pairs, which is capable of encoding a protein of 744 amino acids (Fig. 2B,C). To confirm that the single insertion was responsible for the *ale2* phenotype, we introduced a fragment of genomic DNA that covered the At2g20300 gene into *ale2-1* plants. Plants with the introduced transgene in addition to the homozygous *ale2-1* mutation had a normal phenotype (Fig. 1E). In addition, an independently isolated *ale2-2* mutant that harbored T-DNA within the fifth exon of the At2g20300 gene (Fig. 2B,C) had morphological defects essentially identical to those of *ale2-1* plants (data not shown). We concluded that the At2g20300 gene was equivalent to the *ALE2* gene.

The predicted sequence of the ALE2 protein contains a hydrophobic sequence at the N-terminus and a hydrophobic sequence in the middle region (Fig. 2C). ALE2 also includes an amino acid sequence in the C-terminal region that is strongly conserved in protein serine/threonine kinases (Fig. 2C). These structural features are typical of those of RLKs, and it is likely that the N-terminal region between the two hydrophobic regions serves as the extracellular region. When we used the predicted amino acid sequence of the putative extracellular domain to search available databases, several protein sequences predicted either from cDNA and/or genomic DNA sequences were found to contain sequences significantly homologous to that of ALE2. These sequences were rice XP473126 and XP468388, and *Arabidopsis* At5g56885. All these sequences had a cluster of basic amino acid residues (5-12 residues in each member), followed by sequences containing four cysteine residues (Fig. 2D), which are somewhat similar to that of the processing sites in animal insulin-related peptides. Sequences of these four proteins exhibited significant similarity between the basic region and putative transmembrane domain (Fig. 2D).

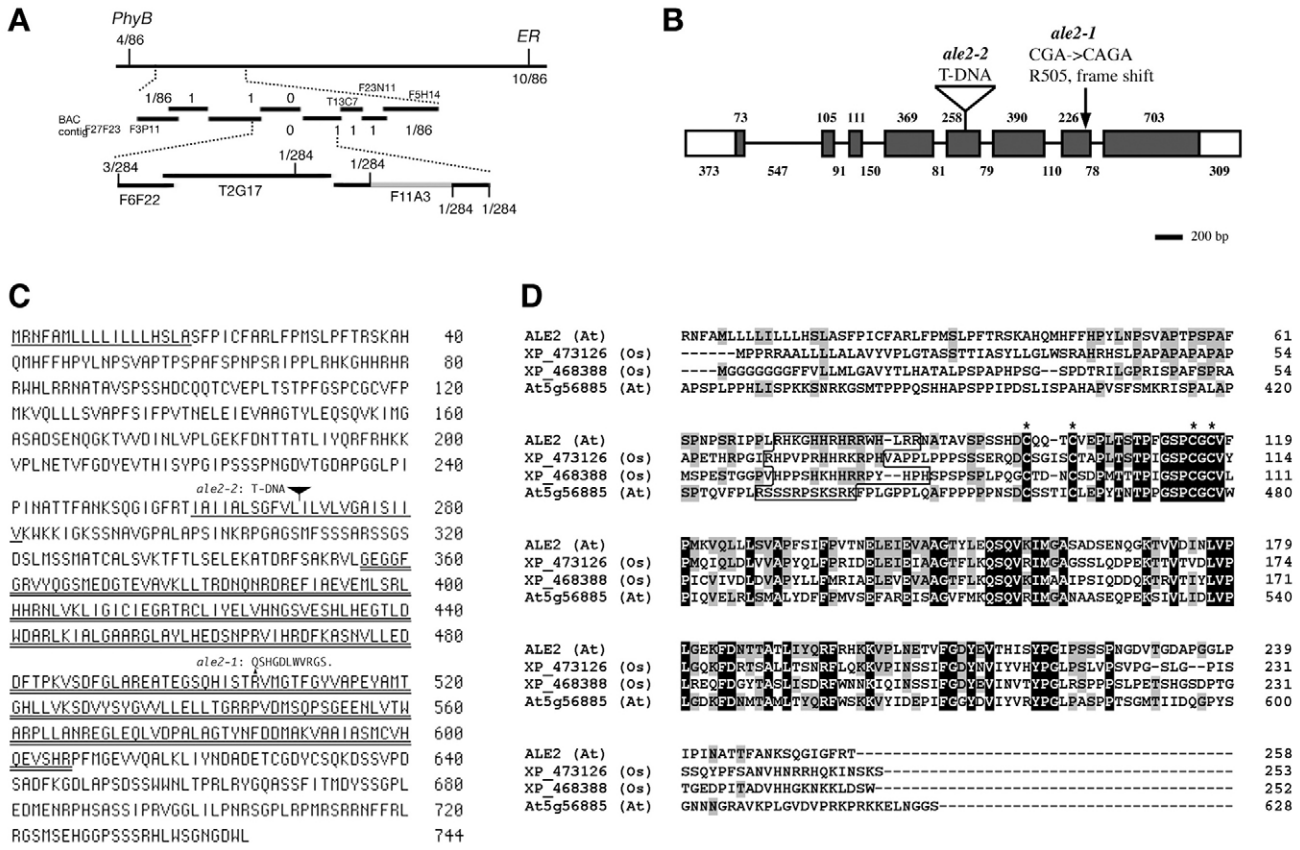

Fig. 2. Map-based cloning and structure of the *ALE2* gene. (**A**) Map position of the *ALE2* gene on chromosome 2. The fractions shown indicate the number of recombinant chromosomes divided by the total number of chromosomes scored for each marker. The 55 kb region between the closest recombination points is indicated as a gray bar. (**B**) Structure of the *ALE2* gene and the positions of mutations. Coding regions and untranslated regions are shown by black and white boxes, respectively. Introns are shown by horizontal bars. The length of each segment is indicated in bp. (**C**) Predicted sequence of the ALE2 protein. Two hydrophobic regions and a kinase domain are indicated by underlining and double underlining, respectively. Mutated amino acid residues in the *ale2-1* allele and sites of T-DNA insertion in the *ale2-2* allele relative to the wild-type amino acid sequence are indicated. (**D**) Comparison of the amino acid sequences of the putative extracellular region of ALE2 and the predicted sequences of other proteins. Clusters of basic amino acid residues are boxed. Positions of conserved cysteine residues are indicated by asterisks.

To examine whether ALE2 is a functional protein kinase, a recombinant protein in which glutathione *S*-transferase (GST) was fused to the putative cytoplasmic region that covered the kinase domain (KD) of the wild-type ALE2 protein (GST:ALE2KD-WT) was synthesized in *E. coli* cells. As a negative control, a mutant fusion protein in which the lysine residue at position 377 in the potential ATP-binding domain was replaced with a tryptophan residue (GST:ALE2KD-KW) was also synthesized. In vitro phosphorylation experiments revealed that the wild-type fusion protein, GST:ALE2KD-WT, had activity to phosphorylate itself and myelin basic protein (MBP), whereas GST:ALE2KD-KW did not (Fig. 3A).

ALE2 and ACR4 mutually increase their phosphorylation in vitro

To gain further insight into the molecular nature of ALE2, we examined whether ALE2 and ACR4, another RLK that is involved in epidermal differentiation (Gifford et al., 2003; Watanabe et al., 2004), could phosphorylate one another. A recombinant protein that contained the putative cytoplasmic region of ACR4 with the protein-kinase domain was synthesized in *E. coli* cells as a histidine- and NusA-tagged fusion (His-Nus:ACR4KD-WT), and was purified. A mutant fusion protein in which the lysine residue in the putative ATP-binding site of ACR4 was replaced with a tryptophan residue (His-Nus:ACR4KD-KW) was also synthesized (Fig. 3B). As shown in Fig. 3C, His-Nus:ACR4KD-WT and GST:ALE2KD-WT proteins phosphorylated the kinase-inactive recombinant proteins GST:ALE2KD-KW and His-Nus:ACR4KD-KW, respectively. When ALE2KD-WT and ACR4KD-WT were used for the reaction, levels of phosphorylation of both proteins significantly increased compared with reactions with either type of kinase-negative proteins (Fig. 3C,D). Thus, ALE2 and ACR4 appear to have the potential to phosphorylate one another.

The *ale2* mutation is semi-dominant in the presence of the *acr4* mutation

The potential biochemical interaction, as well as the similarity between the phenotypes of *ale2* and *acr4* mutants, prompted us to perform phenotypic analysis of an *ale2 acr4* double mutant. We found that *ale2 acr4* plants were viable and able to produce sterile flowers, as was the *ale2* single mutant (Fig. 4A,B). With respect to the number of seeds per silique and the morphology of ovules, the effects of the *acr4* mutation were weaker than those of *ale2*, whereas plants that were double homozygous for the *ale2* and *acr4* mutations

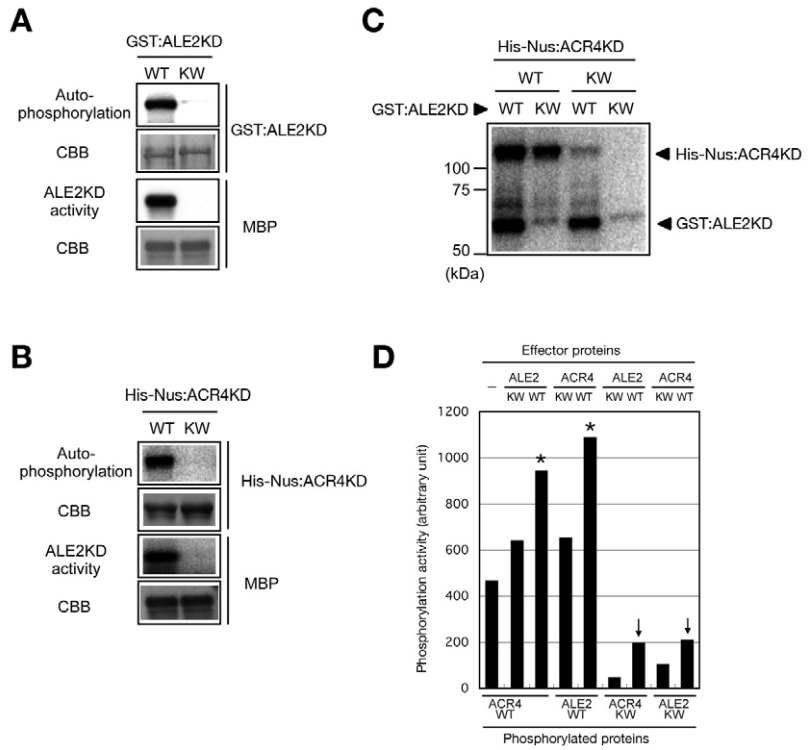

Fig. 3. ALE2 is an active protein kinase. (**A**) In vitro kinase activity of ALE2. GST-fusion proteins of the putative protein kinase domain of ALE2 (GST:ALE2KD) were tested to determine whether they have autophosphorylation activities (upper panel). Kinase activity of GST:ALE2KD was determined with MBP as a substrate (lower panel). (**B**) In vitro kinase activity of ACR4. The His-Nus-fusion protein of the ACR4 protein kinase domain autophosphorylated and phosphorylated MBP in vitro. (**C**) A mutual phosphorylation between ALE2 and ACR4. Effects of ALE2 or ACR4 on the activity of the other kinase were determined by kinase assays in vitro using an equal amount of recombinant ALE2KD and ACR4KD proteins. Four possible combinations of wild-type and kinase-inactive mutant proteins were examined. (**D**) Quantification of phosphorylation activities. The amounts of [γ-^{32}P] ATP incorporated into the substrate proteins were determined. Wild-type ALE2KD and ACR4KD proteins increased the phosphorylation of kinase-inactive ACR4KD and ALE2KD, respectively (arrows). When either wild-type ALE2KD or ACR4KD protein was used as a substrate, a synergistic increase of phosphorylation by the other protein was observed (asterisks).

had a phenotype similar to that of the *ale2* single mutant (Fig. 4A-C). We next examined the phenotypes of plants that were homozygous for one mutation and heterozygous for the other (i.e. *ale2*/+; *acr4* and *ale2*; *acr4*/+). On the homozygous *ale2* mutant background, the effect of a heterozygous *acr4* mutation was unclear (Fig. 4A,B). By contrast, on the *acr4* homozygous mutant background, the effects of the *ale2* mutation were semi-dominant in terms of reduced fertility (Fig. 4B, lanes 7-9).

The *ale1* and *ale2* mutations act synergistically to generate severe epidermal surface defects

We generated plants that were homozygous for the *ale1* and heterozygous for the *ale2* mutation to examine the genetic interaction between *ale1* and *ale2*. Dried seeds obtained from the parental plants included deformed (Fig. 5Aa) and shrunken (Fig. 5Ab) seeds [95 (17.8%) and 48 (9.0%) out of 535 seeds, respectively], which accounted for approximately 25% of all seeds

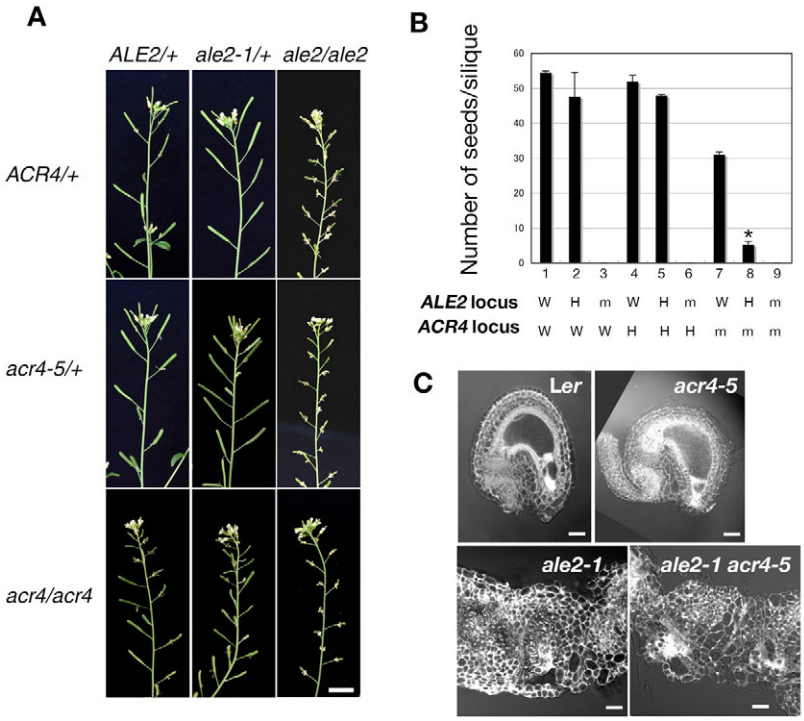

Fig. 4. The *ale2* mutation affects fertility in a semidominant manner in the *acr4* mutant background. (**A**) Inflorescence of self progeny obtained from an *ale2-1*/+; *acr4-5*/+ parent on the L*er* background. Plants that were double homozygous for the *ale2* and *acr4* mutations were viable and resembled *ale2* single-mutant plants. (**B**) Number of enlarged seeds per silique in the progeny of *ale2-2*/+; *acr4-5*/+ plants on the Ws background. Seeds from at least ten siliques were scored for each genotype. The genotype at each locus is indicated. Notice that, whereas *ale2*/+ plants were fully fertile (lanes 2 and 5) in the presence of the wild-type *ACR4* allele, *ale2* mutation affected fertility in a semi-dominant manner in the *acr4* mutant background (indicated by the asterisk above lane 8; compare to lane 7). Essentially the same results were obtained for progeny of *ale2-1*/+; *acr4-5*/+ parents on the L*er* background (data not shown). (**C**) Morphology of ovules. *ale2 acr4* double mutants produced fused ovules that were similar to those of the *ale2* single mutant. W, wild type; H, heterozygous; m, homozygous. Scale bars: 1 cm in A; 20 μm in C.

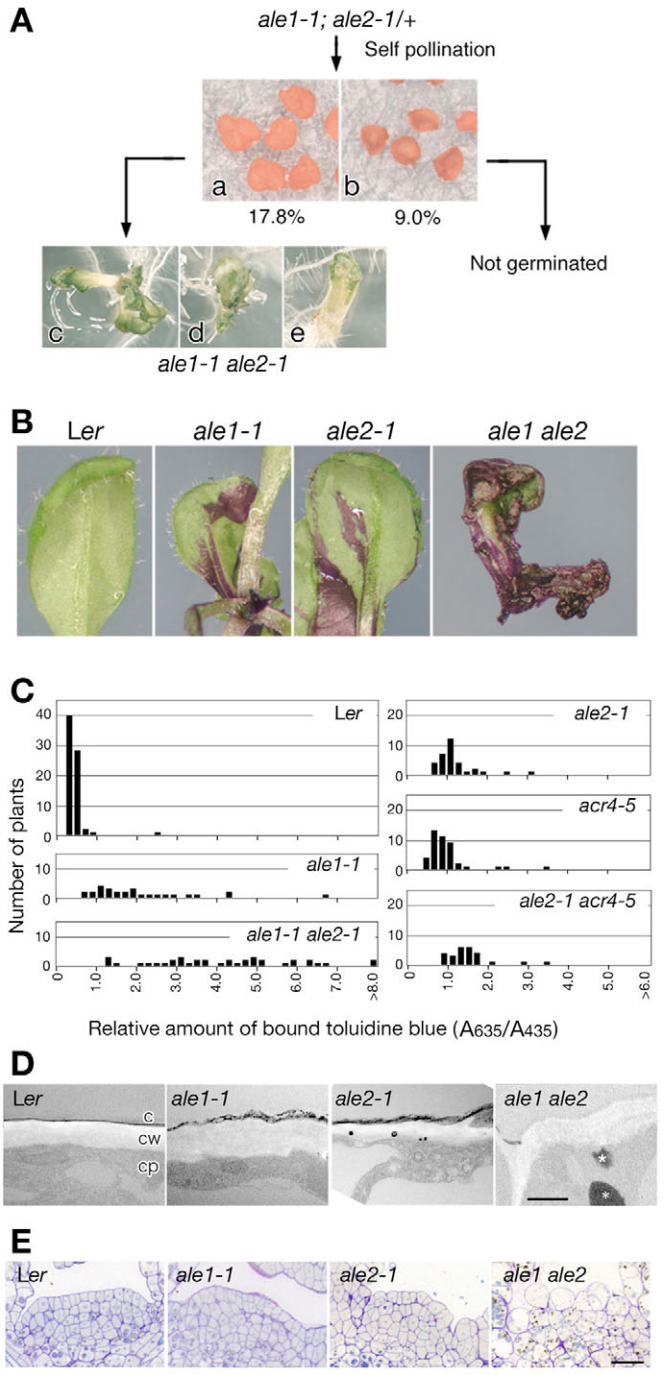

Fig. 5. Synergistic effects of the *ale1* and *ale2* mutations on organ formation and on the formation of leaf cuticle. (**A**) Scheme for the isolation of *ale1 ale2* double mutants. Approximately 25% of seeds from *ale1: ale2*/+ parents were either malformed (Aa) or shriveled (Ab). Seedlings from the malformed seeds had serious morphological defects, to various extents (Ac-Ae). (**B**) Epidermal surface defects verified with TB. Leaves of each single mutant were stained in a patchy pattern. Most of the surface of aerial parts of the *ale1 ale2* double mutant was stained. (**C**) Quantification of the epidermal surface defects in 2-week-old plants by the TB test. (**D**) Transmission electron micrographs showing the surface of epidermal cells. Typical electron-dense granules found in *ale1 ale2* cells are indicated by asterisks. (**E**) Synergistic effects of the *ale1* and *ale2* mutations on shoot organization. Shoot apices of 5-day-old plants are shown. c, cuticle; cw, cell wall; cp, cytoplasm. Scale bars: 1 μm in D; 20 μm in E.

and these phenotypes were rarely observed in the wild type or in single mutants. Shrunken seeds did not germinate, even on solid medium; however, seeds with aberrant morphology germinated, generating seedlings with various degrees of abnormality (Fig. 5Ac-Ae); only a single cotyledon-like structure was present in the most-severely affected cases (Fig. 5Ae). In severely affected seedlings, leaves were formed only after long-term culture or as deformed structures (data not shown). As expected, these seedlings were homozygous for both the *ale1* and *ale2* mutations (data not shown).

Next, we examined the permeability of the leaf surface to TB in single- and double-mutant plants. Wild-type leaves did not allow the dye to permeate their surface (Fig. 5B). Leaves from single mutants were typically stained in a patchy pattern, which suggested the partial loss of cuticle on the surface, as well as the presence of a back-up pathway that was still active and continued to promote cuticle formation (Fig. 5B). Remarkably, the surface of *ale1 ale2* double mutants incorporated significantly more TB (Fig. 5B,C). By contrast, the *ale2 acr4* double-mutant seedlings exhibited a range of epidermal surface defects that were only slightly stronger than, but mainly overlapped those of, the *ale2* single mutant (Fig. 5C). Ultrastructural analysis revealed an enhanced defect in cuticle deposition in *ale1 ale2* double mutants (Fig. 5D). Loss of electron-dense cuticle in *ale1 ale2* double mutants was often associated with the appearance of electron-dense granules in the cytoplasm (Fig. 5D, asterisks).

ALE1 and ALE2 genes are essential for organized development of the protoderm

Because *ale1 ale2* double mutants had impaired epidermal function and impaired organ formation, we postulated that the double mutants might be defective in the differentiation of epidermal precursor cells, which may be important for the formation of leafy organs. To test this hypothesis, we examined the morphology of cells in sections of shoot apices. In sections of wild-type SAM, the L1 layer consists of cells that are relatively regular and rectangular in profile, resulting in the generation of the smooth surface of the SAM (Fig. 5E). The L1 layer in *ale1* or *ale2* single-mutant plants was mainly a single layer of cells (Fig. 5E), whereas, in the shoot apex of *ale1 ale2* double mutants, the outermost cells did not form an organized layer and each cell was swollen, with a rounded appearance (Fig. 5E).

We followed the course of embryogenesis in the wild type and the mutants, focusing on the morphology of protodermal cells and the development of cotyledons. As we reported previously, the *ale1* single mutant was indistinguishable from wild type in terms of the morphology of the embryos before the heart stage (Tanaka et al., 2001) (Fig. 6A,B). In the case of the *ale2* single mutant, we examined embryos obtained from heterozygous parents, because homozygous parents were sterile. We observed a change in the morphology of protodermal cells in approximately 2% of embryos at the globular stage; in these embryos, the protodermal cells were slightly swollen (Fig. 6C,D,E). At the triangular and the heart stages, we observed embryos with a rough surface at frequencies of approximately 13 and 26%, respectively (Fig. 6C,E). In spite of the malformed protodermal cells, *ale2* embryos formed normal cotyledons (Fig. 6C). Morphological defects in embryos were obvious from the globular stage in the case of embryos obtained from *ale1; ale2*/+ parents (Fig. 6D). At the triangular stage and the heart stage, significant fractions of embryos (approximately 13 and 16%, respectively) had very deformed protodermal cells, whose heights were obviously greater than that of anticlinal cell walls of the protoderm (Fig.

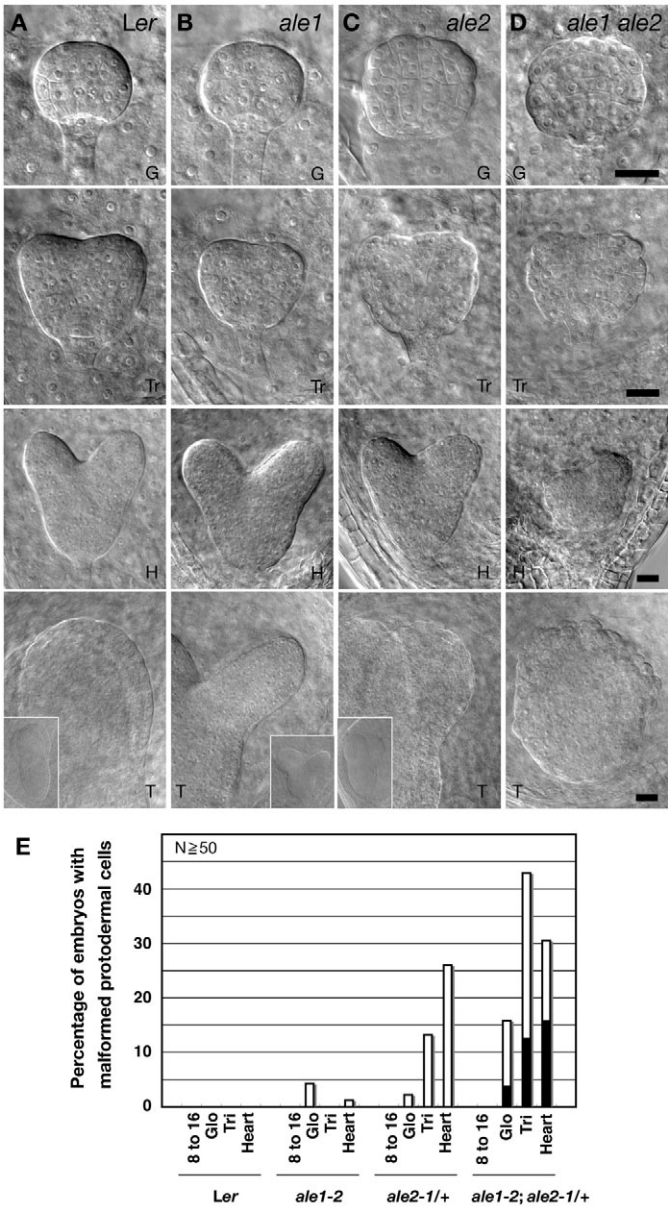

Fig. 6. Defects in cell morphology and organ formation during embryogenesis. (**A-D**) Differential-interference contrast images of cleared embryos of wild-type (*Ler*) (A), *ale1-2* (B), *ale2-1* (C) and *ale1-2 ale2-1* double-mutant (D) embryos. Embryos are shown at the globular (G), the triangular (Tr), the heart (H) and the torpedo (T) stages. The three insets show gross morphology of respective embryos. (**E**) Frequencies of embryos with slightly swollen surfaces (white bars) and nearly spherical protodermal cells (black bars). The abnormal embryos from the indicated parents were scored. Scale bars: 20 μm.

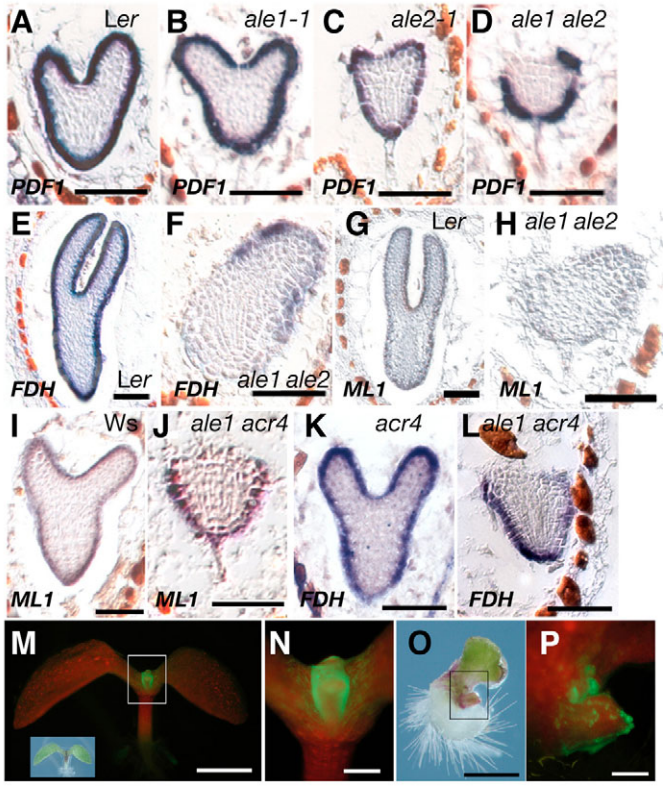

Fig. 7. Defects in *ale1 ale2* and *ale1 acr4* double mutants in the expression of protoderm-specific genes. (**A-L**) Accumulation of *PDF1* (A-D), *FDH* (E,F,K,L) and *ATML1* (G-J) transcripts, as visualized by in situ hybridization of the following embryos: wild type (A,E,G), *ale1-1* (B), *ale2-1* (C) and *ale1-1 ale2-1* (D,F,H) on the *Ler* background; and wild type (I), *acr4-1* (K) and *ale1-1 acr4-1* (J,L) on the Ws background. (**M-P**) 5-day-old seedlings harboring the *pPDF1::GFP* construct. (M) A representative GFP-fluorescence image of a wild-type plant (inset) that expressed the *pPDF1::GFP* construct. (N) Magnified view of the central boxed region in M. (O,P) Gross morphology of an *ale1 ale2* seedling with a disorganized leaf-like structure (O) and disorganized fluorescence due to GFP in the leaf-like organ (P). (P) Corresponds to the boxed area in O. The malformed young leaf exhibits a patchy pattern of fluorescence. Scale bars: 50 μm in A-L; 1 mm in M,O; 200 μm in N,P.

6D,E). As the normal-looking siblings developed to the heart and torpedo stages, the deformation of cotyledons became more obvious, with the occasional loss of bulging of either one or both primordia (Fig. 6D). The frequencies of severe defects in the morphology of protodermal cells were below 25% at all developmental stages (Fig. 6E), suggesting that these phenotypes were present in double-homozygous embryos. However, when mildly affected embryos were taken into account, the percentage of embryos with swollen protodermal cells was more than 25% (Fig. 6E; especially obvious at the triangular stage), perhaps because of a dosage effect of the *ALE2* gene in the absence of activity of the *ALE1* gene.

Patterns of expression of protoderm-specific genes are disrupted in *ale1 ale2* and *ale1 acr4* embryos

The severe functional and morphological defects in the outermost cells in *ale1 ale2* double mutants prompted us to examine whether the mutant embryos had properly specified protoderm. We performed in situ hybridization experiments using probes for various genes that are preferentially expressed in the protoderm. Using probes for transcripts of the *PDF1*, *FDH* and *ATML1* genes, we detected clear signals in the protodermal cells of developing wild-type embryos from the 16-cell through to the torpedo stages (Fig. 7A,E,G,I, and data not shown).

In each single mutant, we detected *PDF1* transcripts in all protodermal cells of heart-stage embryos (Fig. 7B,C). However, in cells in the outermost layer of *ale1 ale2* embryos, the signal was often

below the limit of detection, although strong signals were detected in some outermost cells (Fig. 7D). We obtained similar results after hybridization with *FDH* and *ATML1* probes (Fig. 7E-H). Moreover, when *ale1 ale2* double mutants failed to form one or both cotyledonary primordia, no expression of *FDH* and *ATML1* genes was detectable in the outermost cells in the apical region from which cotyledonary primordia would otherwise have developed (Fig. 7F,H). These results suggest that *ALE2* is required for the specification of protodermal cell fate, for the transcription of protoderm-specific genes and/or for the accumulation of the transcripts of protoderm-specific genes in the absence of *ALE1* activity.

We previously found that *acr4 ale1* double mutants had very severe defects in epidermal surface function and in seedling morphology as compared with each single mutant (Watanabe et al., 2004). To determine whether *ACR4*, like *ALE2*, is responsible for the establishment and/or maintenance of the identity of protoderm in the absence of *ALE1* activity, we examined the expression of protoderm-specific genes in *ale1 acr4* embryos. We failed to detect any hybridization signals due to the *ATML1* and *FDH* probes in the outermost cell layer of the apical region, which included possible sites for the formation of cotyledonary primordia in *ale1 acr4* embryos (Fig. 7I-L). Such abnormal patterns of transcription of the *ATML1* and *FDH* genes in *ale1 acr4* double mutants were similar to those, described above, in *ale1 ale2* embryos.

To gain some insight into the possible mode of regulation of protoderm-specific gene expression by *ALE1* and *ALE2*, we used a *GFP* reporter gene, driven by the *PDF1* promoter (p*PDF1*::*GFP*), and examined its expression in wild-type and *ale1 ale2* double-mutant seedlings. In wild-type seedlings, strong and uniform signals were observed on the surfaces of young leaves (Fig. 7M,N). In *ale1 ale2* seedlings, which had deformed leaves, fluorescence was observed in a patchy pattern on the surfaces of the leaves (Fig. 7O,P).

DISCUSSION

We have described here the isolation and initial characterization of the *ale2* mutant, a novel mutant with defects in morphology and in the functions of epidermal cells. We have shown that the *ALE2* gene encodes a previously uncharacterized RLK, and our results indicate that ALE2 plays an essential role in regulating the differentiation of the protoderm and epidermis in both embryogenesis and post-embryonic development.

ALE2 is a member of a previously uncharacterized RLK/RLCK subfamily

The At2g20300 gene, which turned out to be equivalent to the *ALE2* gene in this study, was originally defined as the gene for a receptor-like cytoplasmic kinase (RLCK), which lacks predicted extracellular domain. Our experiments by RT-PCR and a cDNA sequence from another source (GenBank AY091071) indicated that the *ALE2* gene encodes a protein with a structure typical of RLKs, resembling the majority of members of the *Arabidopsis* RLK gene family (Shiu and Bleecker, 2003). Thus, ALE2 might function as cell-surface receptor. The putative extracellular-domain sequence of the predicted ALE2 protein is similar to that of members of the extensin-like RLK subfamily (Shiu and Bleecker, 2003) (36% and 18% identity to that of the At5g56885 and At4g02010 gene products, respectively). The biological functions of other members in this family are unknown and, thus, ALE2 is unique, at present, insofar as it has a known biological function. Our results suggest that ALE2 might function in the perception and transmission of a signal at the cell surface that is required for the appropriate differentiation and morphogenesis of epidermal cells.

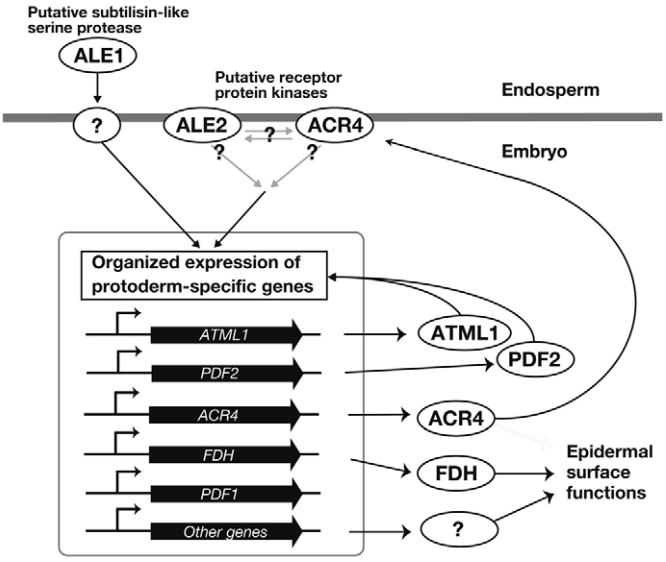

Fig. 8. A putative role for ALE2 in the promotion of protoderm differentiation. The RLK ALE2 and another RLK, ACR4, might function in a single or closely overlapping pathway. ALE1, encoding a putative subtilisin-like serine protease, is predominantly expressed in the endosperm that surrounds the developing embryo (Tanaka et al., 2001) and functions to promote the formation of the protoderm in a manner independent of ALE2 and ACR4. The two pathways involving ALE2, ACR4 and ALE1 might act positively to regulate the specification of the protoderm and/or expression of protoderm-specific genes in an organized manner. The expression of protoderm-specific genes, including those for the ATML1 homeodomain protein and for the redundant factor PDF2, might promote the expression of these genes themselves and other protoderm-specific genes (Abe et al., 2001; Abe et al., 2003). Subsequently, expression of the *FDH* gene for a putative fatty-acid elongase (Yephremov et al., 1999; Pruitt et al., 2000) and of other protoderm-specific genes promotes the formation of the epidermis proper.

A possible mode of ALE2 action in the differentiation of the protoderm

We reported previously that the *ale1* and *acr4* mutations have a synergistic effect on epidermal-surface function, as well as in the formation of cotyledons (Watanabe et al., 2004). These genes encode a putative subtilisin-like serine protease and a RLK, respectively, which both might potentially be involved in intercellular signaling (Tanaka et al., 2001; Tanaka et al., 2002). Because individual mutations seemed to abolish the functions of the encoded proteins, it seems likely that ALE1 and ACR4 can promote the formation of epidermis independently. Our present experiments revealed an effect of the *ale2* mutation that was qualitatively reminiscent of that of *acr4*, although the phenotype of *acr4* was weaker than that of *ale2* (Gifford et al., 2003; Watanabe et al., 2004) (Figs 1, 4). There seemed to be a strict requirement for ALE2 activity in the absence of ACR4, because *ale2* was associated with a semi-dominant phenotype on the *acr4* mutant background (Fig. 4B). In addition, epidermis-related defects in the *ale2 acr4* double mutants were reminiscent of those in the *ale2* single mutant (Figs 4, 5). Taken together, our results suggest the presence of a single or

closely overlapping pathway mediated by ACR4 and ALE2 (Fig. 8). Because ALE2 and ACR4 were able to phosphorylate each other in vitro, a possible model for the mode of their action is that they function as an enzyme-substrate pair in plants, thereby functioning in a single signaling pathway that may promote epidermal specification. In this scenario, their expression patterns should overlap with each other. *ACR4* is expressed in epidermis-related tissues of various organs (Tanaka et al., 2002; Gifford et al., 2003). *ALE2* transcripts appear to be evenly distributed throughout the embryo proper during early embryogenesis, and are preferentially detected both in the outermost cells and in the inner cells of cotyledonary primordia at the early heart stage (see Fig. S1 in the supplementary material). Thus, the pattern of *ALE2* expression is overlapped to some extent with that of *ACR4*. The molecular interaction of these RLKs must, however, be examined by further experiments. Meanwhile, our results support a putative scenario wherein ALE1 functions in a manner that is somehow related to, but is distinct from, the mode of action of ALE2 and ACR4 (Fig. 8). A reasonable hypothesis would be that protoderm specification involves an intertissue communication (i.e. a signal from endosperm that might be generated by ALE1) and an extracellular signaling molecule regulating ALE2 and/or ACR4 activity. Molecular identification and characterization of such molecules would provide further insight into intercellular communication regulating protoderm specification in plants.

Possible mechanism for the regulation of protoderm-specific gene expression and its importance in development

A striking feature of the accumulation of transcripts of protoderm-specific genes in *ale1 ale2* and *ale1 acr4* double mutants was the patchy pattern of such accumulation, with signals as strong as those in wild-type cells in some cells, and below the level of detection in other cells, at the outermost margins of embryos (Fig. 7). A similar patchiness of expression of the p*PDF1::GFP* reporter gene was also observed in leaves (Fig. 7P). These observations suggest that ALE1 and ALE2 might not be absolutely required for the transcription of protoderm-specific genes. Rather, they might be involved in the organized expression of these genes during development. Abe et al. (Abe et al., 2003) proposed that the expression of *ATML1* and *PDF2* might involve self-activating feedback regulation via the L1 box in their promoter regions. Recently, it has been shown that epidermis-specific expression of *ATML1* is controlled by several regulatory sequences in its promoter (Takada and Jürgens, 2007). It is tempting to speculate that ALE1, ALE2 and ACR4 impinge on the activity of such regulatory elements, allowing the uniform expression of protoderm-specific genes. It is increasingly clear that many genes required for the formation of cuticle are expressed in an epidermis-specific manner (reviewed by Tanaka and Machida, 2006; Kurdyukov et al., 2006) and that cuticle is essential for the prevention of the fusion of aerial organs (Tanaka and Machida, 2006). Remarkably, it has been shown that the function of *FDH*, expression of which was seriously affected in *ale1 ale2* and *ale1 acr4* double mutants, is essential for proper leaf surface function [see Lolle et al. (Lolle et al., 1998) and references therein] (Tanaka et al., 2004b). Therefore, it is likely that the severe cuticular defects and organ fusions in *ale1 ale2* and *ale1 acr4* double mutants are due, at least in part, to the impaired expression of protoderm-specific genes, including *FDH*.

In addition, *ale1 ale2* and *ale1 acr4* double mutants were defective in the formation of cotyledons, as is the *atml1 pdf2* double mutant (Abe et al., 2003). Because *ATML1* and *PDF2* are specifically expressed in protodermal cells and are required for the expression of protoderm-specific genes, it is possible that appropriate gene expression in the protoderm is a prerequisite for the formation of cotyledons. Our results suggest that the failure of cotyledon formation in *ale1 ale2* and in *ale1 acr4* double-mutant embryos was associated with a loss of detectable levels of expression of protoderm-specific genes. Another gene that plays a role in the regulation of protoderm-specific gene expression is *AtDEK1* (also known as *DEK1*), which encodes a protein with a calpain-protease domain. The product of this gene is essential for the expression of reporter genes that are driven by the promoters of protoderm-specific genes, such as *ATML1* and *ACR4* (Johnson et al., 2005). In the *atdek1* mutant, development is arrested at the globular stage, without the formation of cotyledons (Johnson et al., 2005). Thus, currently available circumstantial evidence supports the hypothesis that properly differentiated protoderm is somehow essential for the initiation and/or continuous growth of the cotyledons. A further genetic link between the functional differentiation of the epidermis and cotyledon formation has been provided by the analysis of the *gurke* (*gk*; also known as *acc1*) mutant: strong *gk* mutant alleles are associated with the failed formation of cotyledons (Torres-Ruiz et al., 1996; Baud et al., 2004; Kajiwara et al., 2004); and leaky *gk* mutations allow the formation of plantlets but result in the adhesion of aerial organs (Torres-Ruiz et al., 1996) (H. Tanaka and Y.M., unpublished).

In addition to the defect in cotyledon formation, the organization of cell layers in the SAM was severely perturbed in *ale1 ale2* double mutants (Fig. 4E). Such mutants often ceased development after germination, although some eventually generated several small leaf-like organs (Fig. 5A, Fig. 7O). Such morphological and growth defects were associated with the appearance of swollen spherical cells in the outermost layer of the SAM and with a disorganized pattern of expression of the *pPDF1::GFP*. These observations support the hypothesis that proper differentiation of the epidermal cell layer is required for the functions of the SAM and for the subsequent development of leaves. The plant hormone auxin plays a crucial role in the generation of aerial organs (Okada et al., 1991; Reinhardt et al., 2000). The patterns of expression and the subcellular localization of proteins involved in auxin transport indicate that auxin is transported towards the incipient primordia of leafy organs through the protoderm and epidermis (Benková et al., 2003; Reinhardt et al., 2003) (reviewed by Tanaka et al., 2006). Thus, the relationships between the differentiation of the protoderm, the regulation of polar auxin transport, and organ formation might be an interesting topic for future research.

We thank Jirí Friml for enabling H. Tanaka to complete this work in his laboratory. We also thank Yasuo Niwa, the John Innes Centre and the *Arabidopsis* Biological Resource Center for providing materials. The work was supported in part by a Grant-in-Aid for Scientific Research on Priority Areas (no. 14036216) to Y.M., and by a grant for Core Research in Evolutional Science and Technology (CREST) to C.M. from the Japanese Ministry of Education, Science, Culture, Sports and Technology. H. Tanaka was supported by a grant from CREST and was a fellow of the Japan Society for the Promotion of Science (JSPS).

Supplementary material

Supplementary material for this article is available at
http://dev.biologists.org/cgi/content/full/134/9/1643/DC1

References

Abe, M., Takahashi, T. and Komeda, Y. (1999). Cloning and characterization of an L1 layer-specific gene in *Arabidopsis thaliana*. *Plant Cell Physiol.* **40**, 571-580.
Abe, M., Takahashi, T. and Komeda, Y. (2001). Identification of a *cis*-regulatory element for L1 layer-specific gene expression, which is targeted by an L1-specific homeodomain protein. *Plant J.* **26**, 487-494.

Abe, M., Katsumata, H., Komeda, Y. and Takahashi, T. (2003). Regulation of shoot epidermal cell differentiation by a pair of homeodomain proteins in *Arabidopsis*. *Development* **130**, 635-643.
Baud, S., Bellec, Y., Miquel, M., Bellini, C., Caboche, M., Lepiniec, L., Faure, J. D. and Rochat, C. (2004). *gurke* and *pasticcino3* mutants affected in embryo development are impaired in acetyl-CoA carboxylase. *EMBO Rep.* **5**, 515-520.
Benková, E., Michniewicz, M., Sauer, M., Teichmann, T., Seifertova, D., Jürgens, G. and Friml, J. (2003). Local, efflux-dependent auxin gradients as a common module for plant organ formation. *Cell* **115**, 591-602.
Chiu, W., Niwa, Y., Zeng, W., Hirano, T., Kobayashi, H. and Sheen, J. (1996). Engineerd GFP as a vital reporter in plants. *Curr. Biol.* **6**, 325-330.
Cui, Y., Jean, F., Thomas, G. and Christian, J. L. (1998). BMP-4 is proteolytically activated by furin and/or PC6 during vertebrate embryonic development. *EMBO J.* **17**, 4735-4743.
Esau, K. (1977). *Anatomy of Seed Plants*. 2nd edn. New York: John Wiley & Sons.
Gifford, M. L., Dean, S. and Ingram, G. C. (2003). The *Arabidopsis ACR4* gene plays a role in cell layer organisation during ovule integument and sepal margin development. *Development* **130**, 4249-4258.
Hellens, R. P., Edwards, E. A., Leyland, N. R., Bean, S. and Mullineaux, P. M. (2000). pGreen: a versatile and flexible binary Ti vector for Agrobacterium-mediated plant transformation. *Plant Mol. Biol.* **42**, 819-832.
Ito, M., Sentoku, N., Nishimura, A., Hong, S.-K., Sato, Y. and Matsuoka, M. (2002). Position dependent expression of *GL2*-type homeobox gene, *Roc1*: significance for protoderm differentiation and radial pattern formation in early rice embryogenesis. *Plant J.* **29**, 497-507.
Jenik, P. D. and Irish, V. F. (2000). Regulation of cell proliferation patterns by homeotic genes during *Arabidopsis* floral development. *Development* **127**, 1267-1276.
Johnson, K. L., Degnan, K. A., Ross Walker, J. and Ingram, G. C. (2005). *AtDEK1* is essential for specification of embryonic epidermal cell fate. *Plant J.* **44**, 114-127.
Jürgens, G. and Mayer, U. (1994). *Arabidopsis*. In *Embryos: Color Atlas of Development* (ed. J. B. L. Bard), pp. 7-21. London: Wolfe.
Kajiwara, T., Furutani, M., Hibara, K. and Tasaka, M. (2004). The *GURKE* gene encoding an acetyl-CoA carboxylase is required for partitioning the embryo apex into three subregions in *Arabidopsis*. *Plant Cell Physiol.* **45**, 1122-1128.
Krysan, P. J., Young, J. C., Tax, F. and Sussman, M. R. (1996). Identification of transferred DNA insertions within *Arabidopsis* genes involved in signal transduction and ion transport. *Proc. Natl. Acad. Sci. USA* **93**, 8145-8150.
Kurdyukov, S., Faust, A., Nawrath, C., Bar, S., Voisin, D., Efremova, N., Franke, R., Schreiber, L., Saedler, H., Metraux, J. P. et al. (2006). The epidermis-specific extracellular BODYGUARD controls cuticle development and morphogenesis in *Arabidopsis*. *Plant Cell* **18**, 321-339.
Lolle, S. J., Hsu, W. and Pruitt, R. E. (1998). Genetic analysis of organ fusion in *Arabidopsis thaliana*. *Genetics* **149**, 607-619.
Lu, P., Porat, R., Nadeau, J. A. and O'Neill, S. D. (1996). Identification of a meristem L1 layer-specific gene in *Arabidopsis* that is expressed during embryonic pattern formation and defines a new class of homeobox genes. *Plant Cell* **8**, 2155-2168.
Okada, K., Ueda, J., Komaki, M. K., Bell, C. J. and Shimura, Y. (1991). Requirement of the auxin polar transport system in early stages of *Arabidopsis* floral bud formation. *Plant Cell* **3**, 677-684.
Pruitt, R. E., Vielle-Calzada, J. P., Ploense, S. E., Grossniklaus, U. and Lolle, S. J. (2000). *FIDDLEHEAD*, a gene required to suppress epidermal cell interactions in *Arabidopsis*, encodes a putative lipid-biosynthetic enzyme. *Proc. Natl. Acad. Sci. USA* **97**, 1311-1316.
Reinhardt, D., Mandel, T. and Kuhlemeier, C. (2000). Auxin regulates the initiation and radial position of plant lateral organs. *Plant Cell* **12**, 507-518.
Reinhardt, D., Pesce, E. R., Stieger, P., Mandel, T., Baltensperger, K., Bennett, M., Traas, J., Friml, J. and Kuhlemeier, C. (2003). Regulation of phyllotaxis by polar auxin transport. *Nature* **426**, 255-260.
Sasabe, M., Soyano, T., Takahashi, Y., Sonobe, S., Igarashi, H., Itoh, T. J., Hidaka, M. and Machida, Y. (2006). Phosphorylation of NtMAP65-1 by a MAP kinase down-regulates its activity of microtubule bundling and stimulates progression of cytokinesis of tobacco cells. *Genes Dev.* **20**, 1004-1014.
Satina, S., Blakeslee, A. F. and Avery, A. G. (1940). Demonstration of the three germ layers in the shoot apex of Datura by means of induced polyploidy in periclinal chimeras. *Am. J. Bot.* **27**, 895-905.
Shiu, S. H. and Bleecker, A. B. (2003). Expansion of the receptor-like kinase/Pelle gene family and receptor-like proteins in Arabidopsis. *Plant Physiol.* **132**, 530-543.
Stern, C. D. (2005). Neural induction: old problem, new findings, yet more questions. *Development* **132**, 2007-2021.
Takada, S. and Jürgens, G. (2007). Transcriptional regulation of epidermal cell fate in the *Arabidopsis* embryo. *Development* **134**, 1141-1150.
Tanaka, H. and Machida, Y. (2006). The cuticle and cellular interactions. In *Biology of the Plant Cuticle: Annual Plant Reviews.* Vol. 23 (ed. M. Riederer and C. Müller), pp. 312-333. Oxford: Blackwell.
Tanaka, H., Onouchi, H., Kondo, M., Hara-Nishimura, I., Nishimura, M., Machida, C. and Machida, Y. (2001). A subtilisin-like serine protease is required for epidermal surface formation in *Arabidopsis* embryos and juvenile plants. *Development* **128**, 4681-4689.
Tanaka, H., Watanabe, M., Watanabe, D., Tanaka, T., Machida, C. and Machida, Y. (2002). *ACR4*, a putative receptor kinase gene of *Arabidopsis thaliana*, that is expressed in the outer cell layers of embryos and plants, is involved in proper embryogenesis. *Plant Cell Physiol.* **43**, 419-428.
Tanaka, H., Ishikawa, M., Kitamura, S., Takahashi, Y., Soyano, T., Machida, C. and Machida, Y. (2004a). The *AtNACK1/HINKEL* and *STUD/TETRASPORE/AtNACK2* genes, which encode functionally redundant kinesins, are essential for cytokinesis in *Arabidopsis*. *Genes Cells* **9**, 1199-1211.
Tanaka, H., Dhonukshe, P., Brewer, P. B. and Friml, J. (2006). Spatiotemporal asymmetric auxin distribution: a means to coordinate plant development. *Cell. Mol. Life Sci.* **63**, 2738-2754.
Tanaka, T., Tanaka, H., Machida, C., Watanabe, M. and Machida, Y. (2004b). A new method for rapid visualization of defects in leaf cuticle reveals five intrinsic patterns of surface defects in *Arabidopsis*. *Plant J.* **37**, 139-146.
Torres-Ruiz, R. A., Lohner, A. and Jürgens, G. (1996). The *GURKE* gene is required for normal organization of the apical region in the *Arabidopsis* embryo. *Plant J.* **10**, 1005-1016.
Watanabe, M., Tanaka, H., Watanabe, D., Machida, C. and Machida, Y. (2004). The ACR4 receptor-like kinase is required for surface formation of epidermis-related tissues in *Arabidopsis thaliana*. *Plant J.* **39**, 298-308.
Yephremov, A., Wisman, E., Huijser, P., Huijser, C., Wellesen, K. and Saedler, H. (1999). Characterization of the *FIDDLEHEAD* gene of *Arabidopsis* reveals a link between adhesion response and cell differentiation in the epidermis. *Plant Cell* **11**, 2187-2201.